

Air-LUSI: Performance Analysis of a High-Altitude Robotic Telescope used for Tracking the Moon

A. Newton¹, S. E. Maxwell², S. A. Gadsden^{1*}, and K. Turpie³

¹College of Engineering and Physical Science, University of Guelph, Guelph, Ontario, Canada

²National Institute of Standards and Technology, Gaithersburg, Maryland, USA

³University of Maryland Baltimore County, Baltimore, Maryland, USA

*gadsden@uoguelph.ca

Abstract—The air-LUSI (airborne LUnar Spectral Irradiance) mission is a program jointly sponsored by the National Aeronautics and Space Administration (NASA) and the National Institute of Standards and Technology (NIST) that aims to establish the moon as an absolute calibration source for space-based radiometric sensors. Integrated with NASA's high-altitude aircraft, the ER-2, the air-LUSI instrument completed a successful set of so-called Engineering Flights in August of 2018, capturing some of the clearest lunar spectra data sets to date. In response to challenges encountered during the Engineering Flight Campaign, all subsystems, including the Irradiance Instrument Subsystem (IRIS), the Autonomous, Robotic Telescope Mount Instrument Subsystem (ARTEMIS), and High-altitude ER-2 Adaptation (HERA) received upgrades to improve instrument reliability and performance ahead of the 2019 Demonstration Flight Campaign. This paper provides an overview of the project, outlines the upgrades and improvements made to the Autonomous Robotic Telescope Mount Instrument Subsystem (ARTEMIS) by the team at the University of Guelph, and presents the robotic tracking performance data from both the 2018 Engineering and 2019 Demonstration Flight Campaigns.

Keywords—*aerospace; robotics; mechatronic system; tracking system; engineering design; NASA; Earth observations*

I. INTRODUCTION

Space-based optical measuring instruments can be calibrated before launch, but the harsh environmental conditions during launch and on-orbit can cause a change in instrument sensitivity. Common techniques to ensure accurate knowledge of on-orbit sensitivity rely on a combination of intensive pre-launch characterization, as well as the use of solar diffusers, lamp and blackbody sources, viewing of pseudo-invariant sites on earth, and viewing of the moon for in-orbit calibration [1, 2, 3, 4]. These techniques are generally accepted to allow for radiance sensitivity calibrations in the visible and near-infrared at the 2% level and can track trends in sensitivity at the 0.1%/year level [2]. While the moon is already an important part of in-orbit sensor calibration, improved (sub 1% uncertainty)

measurements of its spectral irradiance that tie it directly to the International System of Units (SI) are essential for improving the accuracy of space-based optical radiometric measurements [5, 6].

The best existing model that can provide a predicted lunar irradiance spectrum for a given sun-moon-observer geometry is the Robotic Lunar Observatory (ROLO) Model [7]. This model was developed by the United States Geological Survey (USGS), in partnership with NASA. The measurements which underly the model were made in Flagstaff, Arizona on the USGS campus, which lies at an altitude of about 2,150 meters. The model is believed to have an absolute accuracy at the 5% to 10% level, although it can predict trends with much higher precision. Part of the limit to its accuracy is due to the location: even at this altitude, atmospheric scattering and absorption effects are difficult to quantify and can limit the absolute accuracy of the measurements [5].

While ground-based measurements are expected to play a role in establishing a higher-accuracy lunar spectral irradiance model (for example, NIST is installing a lunar observing station at Mauna Loa Observatory, which is known to have some of the clearest observing conditions on the planet), new measurements from above most of the atmosphere are required to ensure that the new model is not limited by the need to correct for atmospheric conditions. The airborne LUnar Spectral Irradiance (air-LUSI) instrument addresses this need by providing a quasi-Earth based system that is deployed on NASA's high-altitude ER-2 aircraft, and can receive pre-and-post flight calibration. From the vantage point of about 21km, above 95% of the Earth's atmosphere, the incoming lunar spectra are only minimally affected by atmospheric absorption and scattering. The instrument is expected to measure spectra of the moon tied to the SI at the sub 1% level and is a key part of improving on-orbit sensor calibration. The air-LUSI mission is an inter-agency and international NIST- and NASA-sponsored program [8, 9].

To date, the air-LUSI instrument has successfully completed two separate field campaigns [10]. The 2018 Engineering Flight Campaign aimed to prove the engineering efficacy of the device, ensuring safe electromechanical integration with the aircraft, as well as providing a baseline for evaluating the target tracking

capabilities [8]. The 2019 Demonstration Flight Campaign was focused more on demonstrating how well the instrument can achieve its scientific goals, namely, gathering SI-traceable measurements of lunar spectra with an absolute uncertainty sub 1%.

In response to challenges encountered during the Engineering Flight Campaign, all subsystems, including the Irradiance Instrument Subsystem (IRIS), the Autonomous, Robotic Telescope Mount Instrument Subsystem (ARTEMIS), and High-altitude ER-2 Adaptation (HERA) received upgrades to improve instrument reliability and performance ahead of the 2019 Demonstration Flight Campaign. This paper outlines the upgrades and improvements made to ARTEMIS by the team at the University of Guelph, and presents the robotic tracking performance data from the 2018 Engineering and 2019 Demonstration Flight Campaigns.

II. ARTEMIS SUBSYSTEM

The ARTEMIS subsystem comprises a robotic telescope with two linear actuators that drive rotation on a trunnion-supported double gimbal. The design is robust, affordable, and simple. The gimbal allows independent control of the elevation and azimuth of the telescope’s pointing. A machine vision camera is used in conjunction with a tuned control system [9, 11, 12]. The error signal for each actuator is derived from the two axes (labeled x and y) of the camera’s focal plane array. The purpose of the ARTEMIS subsystem is to keep the telescope locked onto the Moon during data acquisition. The systems tracking error is measured by the (x, y) pixel offset from the setpoint in the machine vision camera frame. The total tracking error is represented by the radial offset between the measured Moon center and the setpoint. One pixel of offset corresponds to a 0.053° offset from the target, which is based on the specific camera and lens combination. The mission requirements specify that ARTEMIS keep the moon centered to within 0.5° of the telescopes aperture, or approximately 9 pixels.

III. ENGINEERING FLIGHT CAMPAIGN

In August of 2018, the air-LUSI team deployed to NASA’s Armstrong Flight Research Center (AFRC) for an initial round of flights, called “Engineering Flights.” The team worked on instrument to aircraft integration, pilot and ground crew brief/debriefing sessions, as well as data analysis in the mission control center. The 2018 Engineering Flight campaign aimed at establishing airworthiness and engineering efficacy of the instrument. On the evenings of August 1st and 2nd, the instrument successfully completed two Engineering Flights with tracking performance well within specification for both nights. The following sections provide the tracking performance data from the 2018 Campaign and presents issues that were revealed during instrument operation.

A. Target Tracking Performance

The plots shown in Figs. 1-3 show the Cartesian separation of the target center from the desired pixel setpoint, in the 2D optical plane of the tracking camera, during the Engineering Flight of August 2nd, 2018. This data provides the best metric to quantify the accuracy of the ARTEMIS during the tracking phase of the engineering flight. Over the two-night flight campaign, the design was successful in targeting the Moon with a tracking accuracy that exceeded the 0.5° design constraint by a factor of ten, thereby indicating the effectiveness of the mechanical design and the employed control strategy. Even with this excellent degree of tracking, there were a number of potential risk factors that could lead to a failed mission.

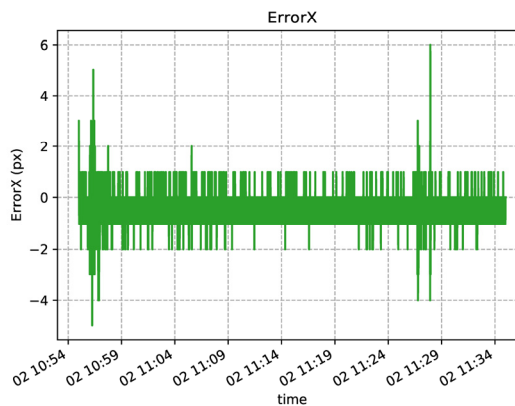


Figure 1. Pixel error in the x-axis [8].

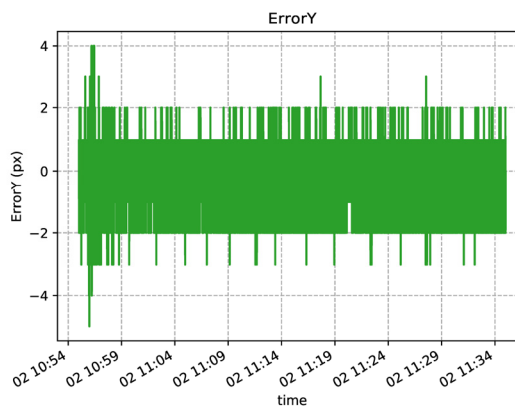


Figure 2. Pixel error in the y-axis [8].

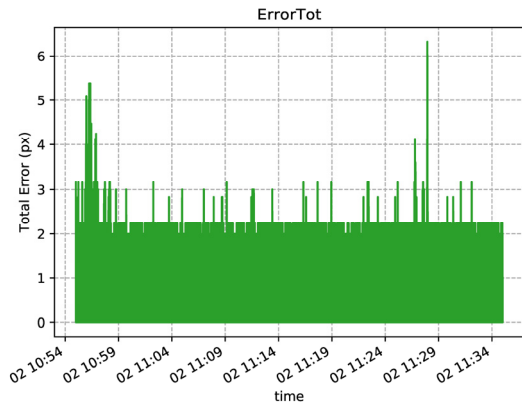


Figure 3. Sample of total pixel error during engineering flights [8].

First, the linear actuators that adjust the telescopes pointing angle were responding to ‘absolute position’ commands, and thus using full power (speed, acceleration, and current) to achieve a given setpoint. This method proved effective for tracking in flight, but led to an overheat failure of the elevation actuator when the air-LUSI instrument was returned to NIST for laboratory calibrations. This indicated a risk of failure in flight. To address this issue, ‘trajectory generated position’ commands replaced the ‘absolute position’ command architecture. The benefit with trajectory generated position commands is that the engineer can define maximum parameters for velocity, acceleration, and torque; such that the control software will generate velocity and acceleration profiles around these parameters that achieve the desired position. By limiting the acceleration to reasonable values, the current and thus the temperature increase in the actuator can be managed. Actuator parameters such as voltage, current, torque, and temperature were added to the data log as a means to monitor the actuator health in flight.

Second, it was discovered that alignment procedure during radiometric calibration routine followed during the Engineering Flights was cumbersome, draining, and in need of some automation. To improve workflow and team dynamics on the hangar floor, an automated spectrometer alignment routine was developed that takes advantage of the motorized scanning capabilities of the ARTEMIS. The result of this automation is an improved workflow, reducing time spent on alignment from 60 minutes down to about 15 minutes.

Third, for accurate tracking of the moon by the telescope, the pixel coordinates on the machine vision camera corresponding to the center of the field of view of the telescope must be identified. For the Engineering Flight Campaign, a laser light source was put at the focus of the telescope and the spot it produced at a range of about 12 meters was identified by the machine vision camera. The known pixel-to-angle conversion factor for the camera along with the measured offset of the camera from the telescope axis was then used to identify the correct pixel coordinates for the center of the telescope field of view. Because this method relied on auxiliary measurements of geometry and relied critically on the alignment of the laser source to the telescope axis, it introduced a risk of error. To

correct for this in the Demonstration Flight Campaign, a bright target was placed at different known distances from the telescope, and at each distance the centroid of the response of the optical system along each axis was determined (by scanning with ARTEMIS). The pixel index of the target in the machine vision frame was recorded at the centroid for each distance, as was the measured distance to the target. Four points were taken to allow a fit and subsequent extrapolation for the expected pixel index on each axis for a target at infinity. These extrapolated indices were taken as the pixel coordinate setpoint for the system in flight.

IV. DEMONSTRATION FLIGHT CAMPAIGN

From October 30th to November 19th of 2019, the air-LUSI team reconvened at AFRC to complete a second round of flights, dubbed the ‘Demonstration Flight Campaign’, consisting of five flights occurring between November 12th-17th. The Demonstration Flight Campaign was focused on illustrating the capability of the instrument to reach its scientific goals: namely, collecting SI-traceable measurements of the lunar spectra with an absolute uncertainty of less than 1%. The following sections provide the tracking performance data from the 2019 Campaign and presents issues that were discovered in the field.

A. Actuator Health and Performance

As a result of adding the actuator health statistics to the data log, it was possible during the 2019 Campaign to monitor the real-time status of the elevation actuator. This was of particular importance since the elevation actuator was considered the highest risk to mission success. Having real-time data such as torque, position, and temperature allowed the mission control team to have eyes on this process and raise a red flag should something go askew. The below figures provide a high-level summary of the actuators’ health and performance during the five-night flight campaign.

Fig. 4 shows an entirely nominal supply voltage for the azimuth actuator over all five nights given that the maximum operating bus voltage is 50V. The elevation actuator was nearly identical and is omitted for brevity. Figs. 5 and 6 illustrate the temperature dynamics of the actuators in flight. The operational temperature range of the actuators is between -40°C and 80°C , and the range seen here is between 20°C and 30°C , showing that both actuators were effectively protected against burn out due to extreme temperatures.

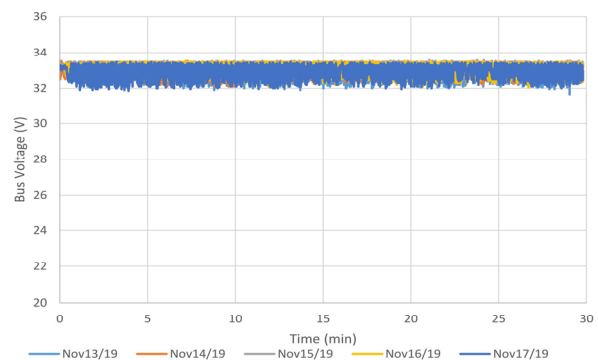


Figure 4. Azimuth actuator bus voltage for demonstration flights.

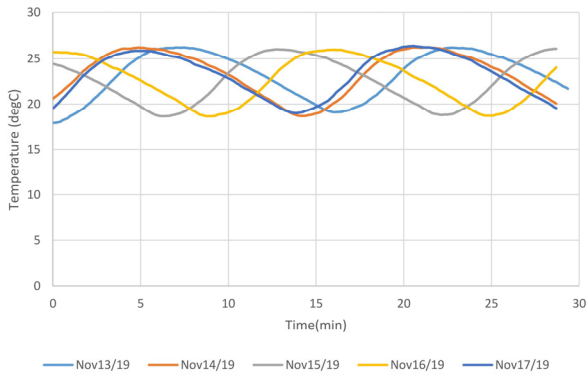


Figure 5. Azimuth actuator temperature throughout flight durations.

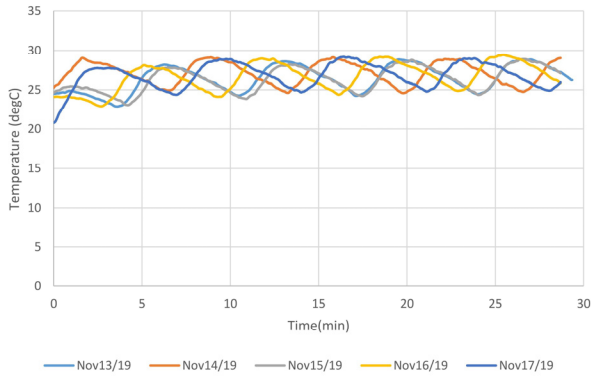


Figure 6. Elevation actuator temperature throughout flight durations.

Figs. 7 and 8 show the angle space range of motions that were achieved by the telescope during tracking. These plots are useful in determining if ARTEMIS was required to traverse to its physical limits, at which point control authority would be lost. Based on the physical design of the instrument and geometric constraints within the science pod of the ER-2, it was found that the maximum range of motion in the azimuthal axis is $\pm 15^\circ$, for elevation angles above 45° . The maximum elevation angle, limited by the actuator length and power demands, is 75° .

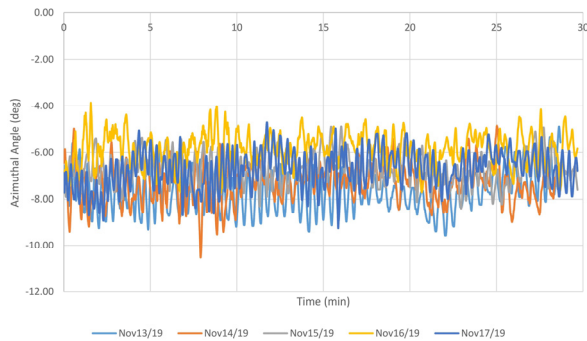


Figure 7. Azimuth actuator range of motion during flights.

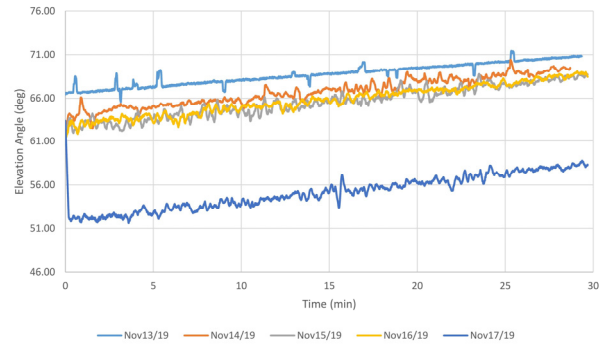


Figure 8. Elevation actuator range of motion during flights.

For brevity, Figs. 9 and 10 show only the actuator torque profile for the November 14th flight. The red lines on the plots indicate the maximum allowable continuous torque, in arbitrary actuator units. Fig. 10 shows a consistent overshoot on this parameter, which is cause for some concern. However, this plot is actually displaying is the instantaneous torque in the actuator, which is flipping between minima and maxima as can be seen more clearly in Fig. 9. The maximum instantaneous torque of the actuator corresponds to a value of 28,000 which was not observed. The data are undersampled, so it is possible that the actuator reached its peak torque, but the data do show that it is likely not a common occurrence during operation. It should be noted that the intense flipping behavior of the torque signal is a direct result of an overloaded actuator. Continued operation in this load regime will lead to increased wear and tear and drastically reduce actuator life.

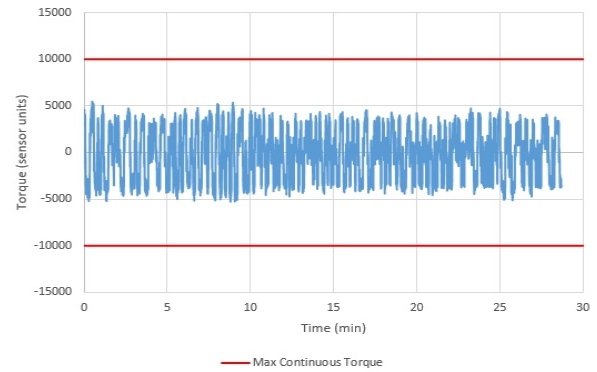


Figure 9. Azimuth actuator applied torque during flight.

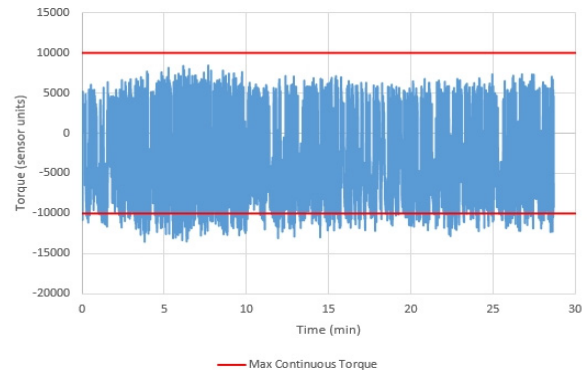


Figure 10. Elevation actuator applied torque during flight.

B. Target Tracking Performance

In the same fashion as the Engineering Flights, the accuracy of the ARTEMIS is evaluated based on the pixel offset from the Moon to the pixel setpoint. The plots below illustrate the tracking accuracy of the ARTEMIS, however in the interest of brevity only the tracking data from the November 14th flight is displayed.

Figures 11 and 12 show the pixel error in the azimuthal and elevation axes, respectively. Interestingly, the elevation actuator, which was the expected culprit of the mission, shows excellent tracking behavior whereas the azimuthal axis is certainly under-performing. Fig. 13 is the absolute, or radial, offset from the Moon center to the pixel setpoint. It can be seen that there were only a handful of instances in which the telescope was completely off target; however, Fig. 14 serves the purpose of providing some context.

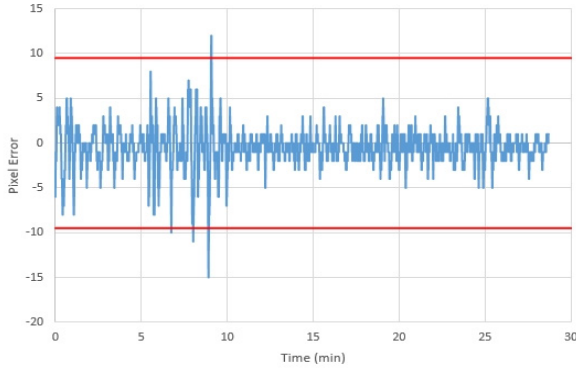


Figure 11. Pixel error in the azimuth axis during flight.

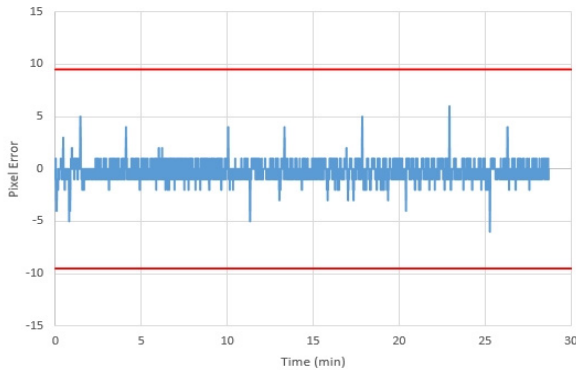


Figure 12. Pixel error in the elevation axis during flight.

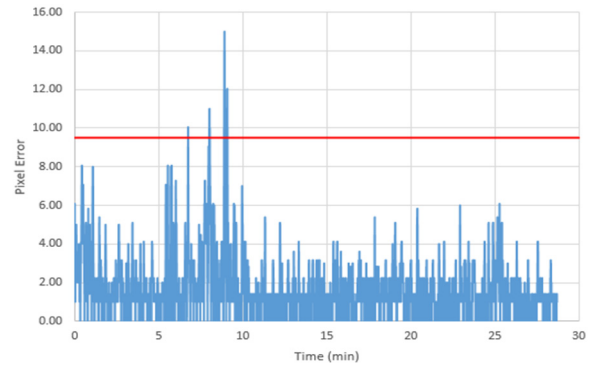


Figure 13. Total pixel error during flight.

Fig. 14 shows the percentage of lunar tracking time that was spent occupying different regimes of accuracy, which are defined in Table 1. It can be seen that even though Fig. 13 shows a few off-target measurements, Fig. 14 illustrates that these off-target measurements only represent 0.4% of the tracking window and can likely be pin-pointed and filtered out. Table 2 provides a concise summary of the tracking data across all five nights and includes the root mean squared error (RMSE) for each night (in terms of degrees).

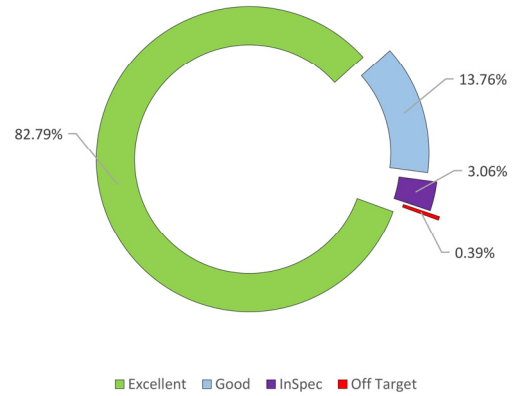


Figure 14. Time spent in different accuracy regimes (%).

TABLE I. THE DIFFERENT REGIMES OF TRACKING ACCURACY

Degree of Accuracy	Total Tracking Error (Degrees)
Excellent	$0 \leq Error < 0.125$
Good	$0.125 \leq Error < 0.25$
In Spec	$0.25 \leq Error < 0.5$
Off Target	$0.5 \leq Error$

TABLE II. SUMMARY OF TRACKING ACCURACY FOR DEMO. FLIGHTS

Range	11/13	11/14	11/15	11/16	11/17
Excellent	76.40%	82.79%	85.74%	83.75%	72.48%
Good	22.01%	13.76%	13.91%	13.31%	23.45%
In Spec	1.54%	3.06%	0.32%	2.91%	3.60%
Off-Target	0.05%	0.39%	0.03%	0.03%	0.38%
RMSE	0.11°	0.11°	0.10°	0.11°	0.13°

C. Response to the Demonstration Flight Campaign

The Moon occupied elevation angles of nearly $61^\circ - 71^\circ$ during flight times, a significant increase from the $50^\circ - 55^\circ$ angle space encountered in the Engineering Flights. From a scientific standpoint, performing these measurements at maximal Moon elevation is ideal since there is less atmosphere for the photons to travel through when the Moon is high in the sky. However, from an engineering standpoint, this not only increases the stress on the robotic control system but also greatly reduces the control authority as the current design is optimized for field of view in the $50^\circ - 55^\circ$ elevation angle space. In other words, as the elevation angle increases, the reachable sight lines of the telescope in the azimuthal axis are greatly reduced. If the team wishes to continue these experiments at near vertical elevation angles, some mechanical redesign of the control system should be explored.

The tracking performance in the azimuthal axis also raised some questions early on in the 2019 Campaign. It was discovered that there was a bug in the flight software where the azimuth actuator was receiving the same acceleration and velocity parameters for the trajectory generation as the elevation actuator. Recall that the elevation actuators acceleration and max velocity was greatly reduced to limit the current drawn by this over loaded motor. The elevation actuator acceleration parameter was set to 100 (arbitrary units) and velocity set to 30,000 (arbitrary units), which proved effective in flight as the elevation actuator only needs to correct for changes in the roll attitude of the aircraft (a fairly stable axis). The azimuth actuator responds to changes in both yaw and pitch of the aircraft, which are far more dynamic. The azimuth actuator was grossly underpowered for the Demonstration Flight Campaign as the correct settings should have been acceleration set to 2,000 and velocity set to 60,000 (based on laboratory and field tests conducted between June and August of 2019). It can also be seen from Fig. 9 that the instantaneous torque never climbed past 5,000 (arbitrary units), thereby indicating that the aforementioned azimuthal acceleration and velocity parameters can be safely implemented.

V. CONCLUSIONS

From October 30th to November 19th of 2019, the air-LUSI team reconvened at NASA's Armstrong Flight Research Center (AFRC) to complete a rigorous flight campaign, consisting this time of five flights occurring between November 12th and 17th. The 2019 Demonstration Flight Campaign was focused primarily on illustrating the capability of the instrument to reach its scientific goals, namely, collecting SI-traceable measurements of the lunar spectra with an absolute uncertainty

of less than 1%. Based on analysis of flight data, it was determined that the Moon was successfully tracked onboard an ER-2 aircraft at an altitude of about 22 km. The accuracy was approximately 0.1 degrees, which was significantly less than 0.5 degrees required to obtain useful calibration data from the Moon as a reference source. Future flight campaigns will look at improving the ARTEMIS system further and obtaining additional data for the calibration science community.

VI. REFERENCES

- [1] R. Barnes, R. Eplee, F. Patt, H. Kieffer, T. Stone, G. Meister, J. Butler and C. McClain, "Comparison of seawifs measurements of the moon with the U.S. geological survey lunar mode," *Journal of Applied Optics*, vol. 43, no. 31, pp. 5838-5854, 2004.
- [2] R. Eplee, R. Barnes, F. Patt, G. Meister and C. McClain, "Seawifs lunar calibration methodology after six years on orbit," in *Proceedings of SPIE: Earth Observing Systems IX*, 2014.
- [3] S. Miller and R. Turner, "A dynamic lunar spectral irradiance data set for npoess/viirs day/night bandnighttime environmental applications," *IEEE Transactions on Geoscience and Remote Sensing*, vol. 47, no. 7, pp. 2316-2329, 2009.
- [4] X. Xion, J. Sun, J. Fullbright, Z. Wan and J. Butler, "Lunar calibration and performance for s-npp viirsreflective solar bands," *IEEE Transactions on Geoscience and Remote Sensing*, vol. 54, no. 2, pp. 1052-1062, 2016.
- [5] T. Stone and H. Kieffer, "Use of the moon to support on-orbit sensor calibration for climate change measurements," in *Proceedings of SPIE: Earth Observing Systems XI*, 2006.
- [6] J. Sun, R. Eplee, X. Xiong, T. Stone, G. Meister and C. McClain, "MODIS and SeaWIFS on-orbit lunar calibration," USGS, 2008.
- [7] T. Stone and H. Kieffer, "Absolute irradiance of the moon for on-orbit calibration," in *Proceedings of SPIE: Earth Observing Systems VII*, 2002.
- [8] A. Cataford, "Air-LUSI: The Mechanical and Control System Design of NASA's Airborne Lunar Observatory," University of Guelph, Guelph, Ontario, 2018.
- [9] A. Cataford, S. A. Gadsden and K. R. Turpie, "Air-LUSI: Autonomous telescope design for lunar spectral irradiance measurements," in *SPIE Advanced Optics for Imaging Applications: UV through LWIR IV*, Baltimore, Maryland, 2019.
- [10] A. Cataford, S. A. Gadsden and K. Turpie, "Air-LUSI: A robotic telescope design for lunar spectral measurements," *Advances in Space Research*, vol. 65, no. 10, pp. 2315-2323, 2020.
- [11] A. Cataford, S. A. Gadsden, K. R. Turpie and M. Biglarbegian, "Air-LUSI: Estimation, Filtering, and PID Tracking Simulation," in *IEEE Canadian Conference on Electrical and Computer Engineering (CCECE)*, Quebec City, Quebec, 2018.
- [12] S. A. Gadsden, "An Adaptive PID Controller Based on Bayesian Theory," in *ASME Dynamic Systems and Control Conference*, Tysons Corner, Virginia, 2017.